

<https://doi.org/10.1590/2318-0331.282320230018>

Turbulent pressures at the position of maximum pressure fluctuation in hydraulic jump stilling basins

Pressões turbulentas na posição de flutuação de pressão máxima em bacias de dissipação por ressalto hidráulico

Renato Steinke Júnior¹ , Priscila Maria Kipper¹ , Leandro Broch Ferreira¹ , Eder Daniel Teixeira¹ ,
Maurício Dai Prá¹  & Marcelo Giulian Marques¹ 

¹Universidade Federal do Rio Grande do Sul, Porto Alegre, RS, Brasil

E-mails: renato.steinkejunior@gmail.com (RSJ), priscila.kipper@ufrgs.br (PMK), leandro.broch@acad.pucrs.br (LBF), eder.teixeira@ufrgs.br (EDT), mauricio.daipra@ufrgs.br (MDP), mmarques@iph.ufrgs.br (MGM)

Received: December 18, 2022 - Revised: March 21, 2023 - Accepted: April 28, 2023

ABSTRACT

Turbulent flow is responsible for a significant portion of damages and failures in dams. This paper sought to introduce novel approaches to the estimation of typical parameters used in the design of stilling basins. The standard deviations of pressure samples of 24 hydraulic jumps were analysed throughout the stilling basin longitudinal centreline, and the positions of maximum pressure fluctuation were identified. Next, mean and extreme pressures occurring at this position were calculated. Finally, these parameters were plotted against the inflow Froude number and curves were adjusted to the data. The position where maximum turbulence of undular, weak and oscillating jumps occurs varies according to the Froude number. Steady and strong jumps are more likely to induce negative pressures on the stilling basin. The findings of this paper broaden the knowledge on which regions of the stilling basin must receive special attention, and on how to minimize the chances of damages.

Keywords: Extreme pressures estimation; Position of maximum pressure fluctuation; Hydraulic structures; Stilling basins; Hydraulic jump.

RESUMO

O escoamento turbulento é responsável por diversos danos e falhas nas barragens. Neste artigo, introduz-se uma abordagem para estimar parâmetros característicos do dimensionamento de bacias de dissipação. Os desvios padrão das amostras de pressão de 24 ressaltos hidráulicos foram analisados em todo o eixo longitudinal da bacia de dissipação, e as posições de flutuação de pressão máxima foram identificadas. Em seguida, foram calculadas as pressões médias e extremas que ocorrem nesta posição. Finalmente, estes parâmetros foram plotados em relação ao número de Froude incidente e foram ajustadas curvas aos dados. A posição onde ocorre a máxima turbulência de ressaltos ondulados, fracos e oscilantes varia de acordo com o número de Froude. Ressaltos firmes e fortes são mais propensos a gerarem pressões negativas na bacia de dissipação. As conclusões ampliam o conhecimento sobre quais regiões da bacia de dissipação devem receber atenção especial e como minimizar as chances de danos.

Palavras-chave: Estimativa de pressões extremas; Posição de flutuação de pressão máxima; Estruturas hidráulicas; Bacias de dissipação; Ressalto hidráulico.

INTRODUCTION

Hydraulic jump stilling basins are structures frequently present in dams, with the purpose of dissipating the energy contained in the surplus flow and safely restituting this water volume to the natural river stream. This energy dissipation is required in order to protect the riverbed against progressive erosion that could compromise the foundations and, consequently, the dam safety. Due to the great hydraulic energy that dams can store, stilling basins, which are subjected to the effects of a highly turbulent flow, must be capable of withstanding sudden pressure and velocity oscillations, which impose significant loads on the structure. In a hydraulic jump, the energy is dissipated mainly through the development of intense turbulence, characterized by high pressure and velocity variations and by the emergence of large eddies, that develop in further vortices of lesser magnitude until, finally, the turbulent energy is converted into heat (Bowers & Toso, 1988; Mees, 2008). The characterization of these intense pressure and velocity fluctuations is fundamental to the design of safe and economical energy dissipators.

Hydraulic jumps have been piquing the technical-scientific community's curiosity for years, and are still to the present day an object of study. Recent examples are the works of Barjastehmaleki et al. (2016) and Maleki & Fiorotto (2021), that contain recommendations on the design of hydraulic jump stilling basins. As the computational power increases, the researches involving the numerical modelling of the hydraulic jump are gaining visibility, some examples being Jesudhas et al. (2018), Witt et al. (2018) and Macián-Pérez et al. (2020).

The study of extreme pressures on the bottom of stilling basins began with the development of pressure transducers, in the 1960s. This knowledge is necessary for the structural design of the stilling basin, its bottom slabs, anchoring, etc. (Fiorotto and Rinaldo, 1992; Fiorotto and Salandin, 2000). Due to the jump's inherent turbulence, it is not possible to analytically determine the loads transmitted to the basin, which is why statistical analysis is the classical approach when studying pressure fluctuations. The studies of Stojnic et al. (2021), Hassanpour et al. (2021) and Steinke Júnior et al. (2021) analyse statistical parameters of instantaneous pressure samples collected in hydraulic jump physical models, such as the mean, the standard deviation, extreme values and third and fourth order moments, among others.

The inflow Froude number F_1 is a determinant parameter in the study of hydraulic jumps, and may be understood as the relationship between the inertial and gravitational forces (Equation 1).

$$F_1 = \frac{v_1}{\sqrt{g y_1}} \quad (1)$$

in which v_1 is the average incident velocity (m/s); y_1 is the supercritical sequent depth (m); g is the acceleration due to gravity (m/s²).

In a Report published in the 1950s, Bradley & Peterka (1955) established that the hydraulic jump could be classified in at least four different types, according to the inflow Froude number. The information contained in this and in other Reports was later used to assemble Monograph 25 (Peterka, 1984), first published in 1958. Chow (1959) and Elevatorski (1959) also contain very similar classifications. Apart from some minor terminology differences, the jump forms are: undular, weak, oscillating, steady and strong,

as shown in Figure 1. Generally speaking, the higher the Froude number, the higher the ratio between the sequent depths, the stronger the turbulence and the higher the energy dissipation H_t (Figure 2). The undular jump (Figure 1a) is characterized by small superficial perturbances and a sequent depth ratio close to unity. In weak jumps (Figure 1b), small rollers develop near the upstream surface. Energy dissipation is less than 20%. The oscillating jump (Figure 1c) usually occurs in low head dams and is characterized by a jet that oscillates from the bottom to the surface, generating irregular period waves that may travel through long distances and damage earth banks and riprap. The steady or well-stabilized jump (Figure 1d), which provides an energy dissipation between 45% and 70%, is named after the fact that its positioning and functioning are relatively unresponsive to tailwater oscillations. For Froude numbers higher than 9.0 (strong jump, Figure 1e) the inflow sequent depth becomes relatively small, as the inflow velocity rises. Although the energy dissipation may reach up to 85%, this type of jump is not recommended in hydraulic structures due to potential risks of erosion and cavitation on the concrete (Chow, 1959; Peterka, 1984; Teixeira, 2008).

According to Toso & Bowers (1988), the damages found in stilling basins are caused mainly by the pressure fluctuations, that were addressed in several works comprising hydraulic jumps: Vasiliev & Bukreyev (1967), King (1967), Bowers & Tsai (1969), Abdul Khader & Elango (1974), Akbari et al. (1982), Lopardo (1986), among others. Marques et al. (2017) list several types of damage that can occur in hydraulic structures: cavitation, abrasion, erosion, cracks, vibration-related damages, structural instabilities, hydraulic transient, etc.

Pfister & Hager (2010) affirm that the 1960s and the 1970s were marked by several serious damages in spillways and auxiliary appurtenances. A great amount of these damages was caused by cavitation, one example being the Keban Dam, in Turkey. The high velocities and the flow impact on the structure eroded the concrete along the bottom of the discharge channel, as shown in Figure 3. One way to avoid cavitation is through the flow aeration (Pfister & Hager, 2010). To solve the problem of Keban Dam, four aeration shafts were installed along the discharge channel, using special techniques to demolish the existent concrete (TEMELSU, 2022).

According to Toso & Bowers (1988), it was common practice to use extreme pressures with a probability of occurrence of 1% on the design of stilling basins. The authors argued that such a probability is not sufficiently conservative and recommended the use of even more extreme pressures. Lopardo (1985) made the same recommendation, stating that the pressures with a probability of non-exceedance of 0.1% are the ones that best represent the tendency to instantaneous cavitation. This was validated by the study of Lopardo (2002), conducted with experimental data from both prototype and physical model.

Steinke Júnior et al. (2021) analysed the minimum pressures of low Froude number hydraulic jumps. The authors verified that this type of jump behaves differently than steady jumps, as shown in Figure 4a. The differences were mostly attributed to the oscillating jet beneath the roller. Furthermore, the oscillating jet in low Froude number hydraulic jumps affects the pressure fluctuations, which also behave differently than steady jumps, as shown in Figure 4b (the variables $\Psi_{0.1\%}$ and Ω will be defined

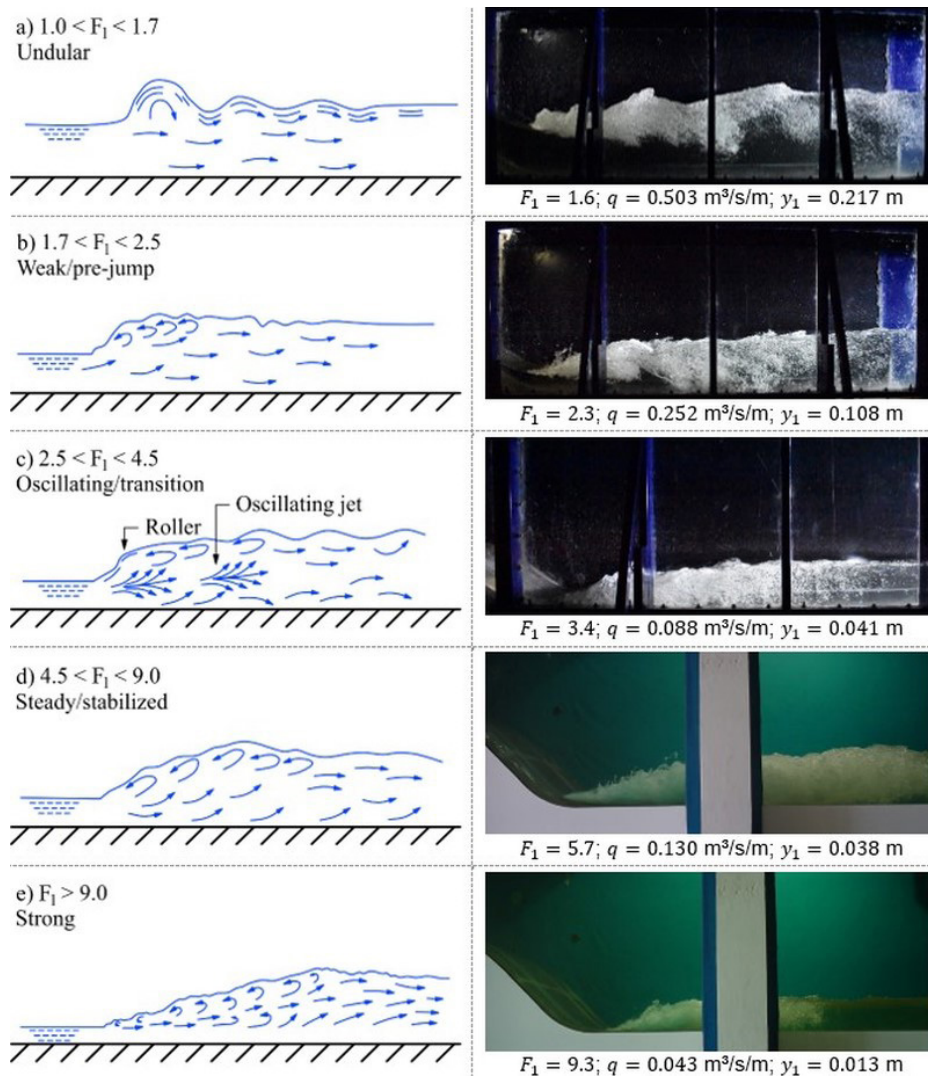


Figure 1. Hydraulic jump forms. Illustrations adapted from Peterka (1984) and Teixeira (2008). Photos taken by Dai Prá (2011) and Steinke Júnior (2020).

later). These differences motivate the investigations on the effects of the Froude number over the statistical parameters calculated from the instantaneous pressures exerted by the jump on the stilling basin apron.

Thus, as an attempt to expand the comprehension on the pressure field acting on the slabs of hydraulic jump stilling basins, and also as a contribution to decrease the occurrence of damages and failures such structures, the present paper aims at proposing novel approaches to practically determine the mean pressures, the minimum and maximum extreme pressures, the maximum fluctuations along hydraulic jumps and the position where they occur.

MATERIAL AND METHODS

The data series of instantaneous pressures used in this study were experimentally collected by independent researchers in different laboratories, using pressure transducers in physical models of hydraulic jump stilling basins.

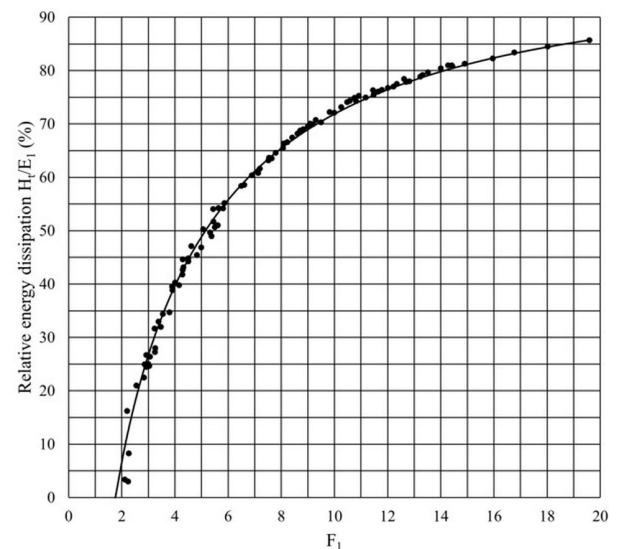


Figure 2. Energy dissipation as a function of the Froude number. Adapted from Peterka (1984).



Figure 3. Cavitation induced damages in Keban Dam. Şentürk (1994).

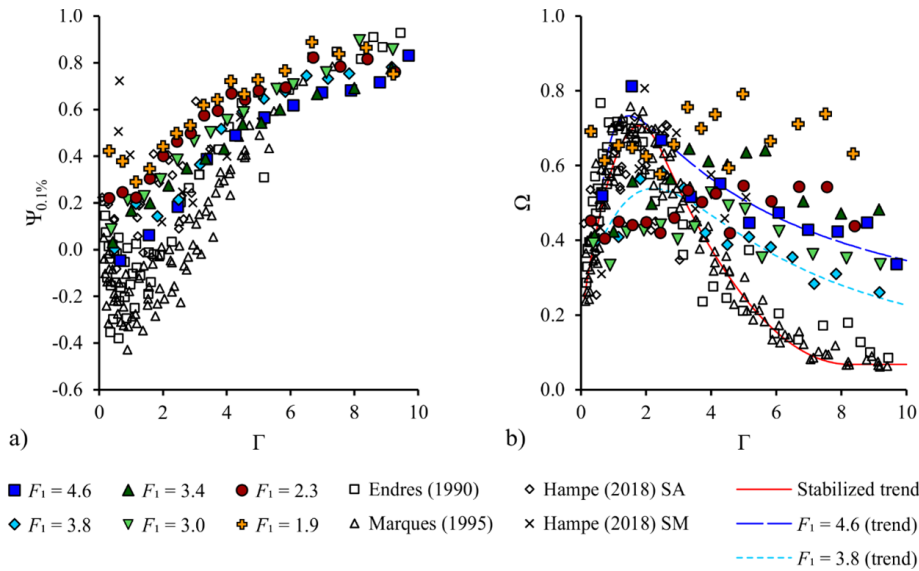


Figure 4. (a) Dimensionless minimum pressures and (b) dimensionless pressure fluctuations as a function of the longitudinal position. Steinke Júnior et al. (2021).

Endres (1990) studied free hydraulic jumps with five different Froude numbers (ranging from 4.2 to 8.6) on a model installed at the Institute of Hydraulic Research – Universidade Federal do Rio Grande do Sul (UFRGS), in Porto Alegre, Brazil (Figure 5a). The experimental installation consists of a 0.72-m-tall spillway followed by a stilling basin installed in a 0.72-m-wide and 15-m-long channel. Along the stilling basin, 11 pressure transducers were installed to collect pressure values with a 100 Hz frequency during 100 s.

Marques (1995) used an experimental installation corresponding to a 0.60-m-wide and 12-m-long, equipped with a 0.72-m-tall spillway, built in the Laboratoire d'Hydraulique du Département de Génie Civil de l'Université Laval, in Québec, Canada (Figure 5b). The pressure samples were collected with a frequency of 50 Hz during 200 s using 22 transducers along the channel longitudinal axis. The six experimental runs comprised Froude numbers ranging from 4.9 to 9.3. It is worth mentioning that the spillway crest obeys the same equation of the experimental setup used by Endres (1990).

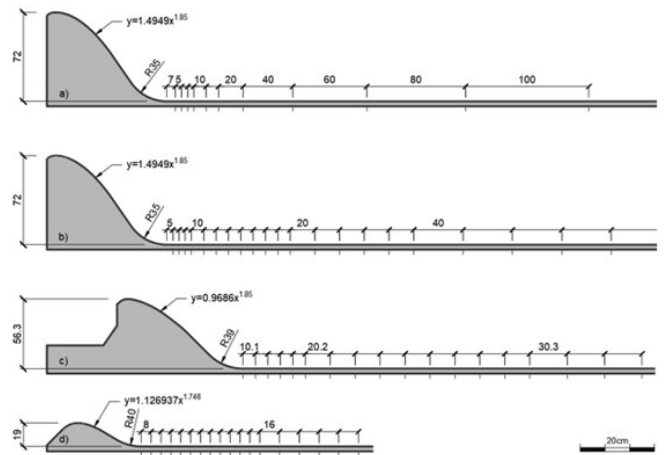


Figure 5. Longitudinal cross section of experimental models: (a) Endres (1990); (b) Marques (1995); Dai Prá (2011) and (d) Steinke Júnior (2020).

Table 1. Test conditions of the data samples used in this study.

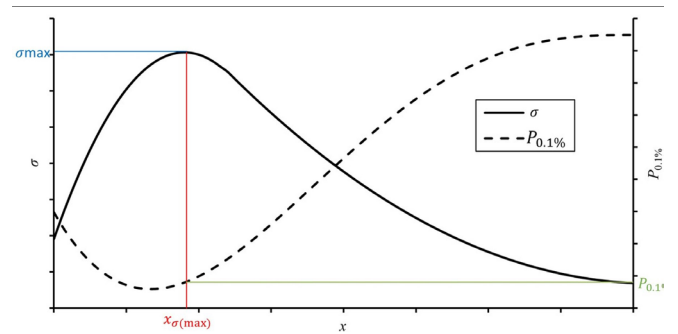
Study	Range of F_1	No. of runs	Acquisition frequency (Hz)	Sample duration (s)	Spillway approach height (m)
Endres (1990)	$4.2 < F_1 < 8.6$	5	100	100	0.72
Marques (1995)	$4.9 < F_1 < 9.3$	6	50	200	0.72
Dai Prá (2011)	$4.4 < F_1 < 9.3$	6	500	600	0.56
Steinke Júnior (2020)	$1.6 < F_1 < 4.6$	7	100	600	0.19

Dai Prá (2011) collected pressure data in an experimental model of a stilling basin downstream of a spillway, built in LAHE (Portuguese acronym for Water Resources and Experimental Hydraulics Laboratory), Rio de Janeiro, Brazil (Figure 5c). The experiments covered hydraulic jumps within the range $4.4 < F_1 < 9.3$ and submergence factors with $1.00 < S < 1.73$. In the present study, however, only the data collected from hydraulic jumps with $S=1.00$ were used, i. e., A-jumps (also called free jumps). The 1.150-m-wide channel was equipped with a spillway representing, on a 1:32 scale, the one present in Porto Colômbia HPP (Hydroelectric Power Plant). Fourteen transducers, installed along the centreline of the stilling basin and part of the spillway, were used to register instantaneous pressure data with a 500 Hz rate during 600 s.

Steinke Júnior (2020) used an experimental installation present at the Laboratory of Hydraulic Works of the Institute of Hydraulic Research, UFRGS, Porto Alegre, Brazil (Figure 5d). The model consists of a 15.5-m-long, 0.395-m-wide and 0.80-m-high channel. The spillway, with a height of 0.19 m and a longitudinal length of 0.78 m at its base, represents, on a 1:50 scale, the one present at Santo Antônio HPP, in Porto Velho, Brazil. Although the prototype spillway has 15 gates, the model was deliberately conceived with none. Along the longitudinal axis of the channel, 23 pressure transducers were installed, registering data with a frequency of 100 Hz during 600 s. The seven test runs performed comprised undular, weak and oscillating jumps ($1.6 < F_1 < 4.6$).

It is important to point out that the aforementioned data are from studies independently carried out by different researchers in different laboratories, throughout three decades, having in common exclusively the fact of being conducted in type I stilling basins, with A-jumps. Table 1 contains a summary of the data samples collected by each one of the mentioned authors. Depending on the considered source, the pressure data present different sampling criteria. Teixeira (2008) recommends minimum acquisition frequency of 50 Hz and minimum sampling duration of 600 s for laboratory studies aiming to characterize the hydraulic jump pressure field acting on stilling basins. Despite the sampling durations of the datasets from Endres (1990) and Marques (1995) being shorter than the recommended value, the pressure statistics taken from these data are consistent with each other and with data from other studies and, thus, was considered suited for the analyses here carried out. As for the acquisition frequency, all four datasets fall within the recommended limit.

Finally, besides the already mentioned data, results from Abdul Khader & Elango (1974), Toso & Bowers (1988) and Lopardo (1986) were also included in the analyses. These data were not used to derive the equations here introduced, but for comparison and validation only.

**Figure 6.** Example of determination of the parameters σ_{max} , $x_{\sigma(max)}$ and $P_{0.1\%}$.

The standard deviations (herewith also called pressure fluctuation) throughout the stilling basin were calculated for each data sample. Then, the maximum pressure fluctuations σ_{max} of each sample were identified, together with the longitudinal position where they occurred $x_{\sigma(max)}$. Finally, the mean pressure \bar{P} and the quantiles 0.1% and 99.9% of the probability distribution ($P_{0.1\%}$ and $P_{99.9\%}$, respectively) were calculated at this position, according to the recommendations from Lopardo (2002). The variables $P_{0.1\%}$ and $P_{99.9\%}$ will be respectively referred to as extreme minimum and maximum pressures throughout this paper. Figure 6 is an example of the determination of these parameters for a generic Froude number. The mean pressures \bar{P} and the maximum pressures $P_{99.9\%}$ were determined similarly to $P_{0.1\%}$.

The mean, minimum and maximum pressures, as well as the maximum fluctuations and the positions where they occurred were nondimensionalized as in Steinke Júnior (2020), also as suggested by Marques et al. (1997), according to Equations 2, 3, 4, 5 and 6, respectively. Additionally, the pressure fluctuation coefficient given by Equation 7 was used to analyse this parameter.

$$\Psi = \frac{\bar{P} - y_1}{y_2 - y_1} \quad (2)$$

$$\Psi_{0.1\%} = \frac{P_{0.1\%} - y_1}{y_2 - y_1} \quad (3)$$

$$\Psi_{99.9\%} = \frac{P_{99.9\%} - y_1}{y_2 - y_1} \quad (4)$$

$$\Omega_{max} = \frac{\sigma_{max}}{H_t} \frac{y_2}{y_1} \quad (5)$$

$$\Gamma_{\sigma(max)} = \frac{x_{\sigma(max)}}{y_2 - y_1} \quad (6)$$

$$C'_p = \frac{\sigma_{\max}}{\frac{v_1^2}{2g}} \quad (7)$$

where \bar{P} is the dimensional mean pressure, in equivalent head, at the position of maximum pressure fluctuation (m); $P_{0.1\%}$ and $P_{99.9\%}$ are the dimensional extreme pressure quantiles for the probabilities 0.1% and 99.9%, in equivalent head, at the position of maximum fluctuation (m); v_1 and v_2 are the sequent depths (m); σ_{\max} is the maximum pressure fluctuation, in equivalent head (m); H_t is the energy dissipated along the jump, in equivalent head (m); $x_{\sigma(\max)}$ is the position where the maximum pressure fluctuation occurs (m); ψ is the dimensionless mean pressure; $\Psi_{0.1\%}$ and $\Psi_{99.9\%}$ are the dimensionless extreme pressure quantiles for the probabilities 0.1% and 99.9%; Ω_{\max} is the dimensionless maximum pressure fluctuation; C'_p is the maximum pressure fluctuation coefficient; $\Gamma_{\sigma(\max)}$ is the dimensionless position where the maximum pressure fluctuation occurs.

The dimensionless values of the mean, minimum and maximum pressures, as well as the maximum pressure fluctuations and the position where they occurred were plotted against the Froude numbers of each data samples. Trendlines were adjusted using the least squares method. The charts of Figure 7 to 13 contain the data points and the fitted curves, as well as the 95% Confidence Band (CB95%) for the respective equation. It is important to highlight that the derived equations are valid only for the range of Froude numbers comprised by the data samples used: $1.6 < F_1 < 9.3$.

RESULTS AND DISCUSSIONS

Maximum pressure fluctuation

The results found for the dimensionless maximum standard deviation Ω_{\max} of the data samples, herewith also called maximum pressure fluctuations, plotted against the Froude number, are shown in Figure 7. The data points present a sharp decrease with respect to the Froude number for $F_1 < 3$. For Froude numbers above this value, the function increases. This difference is attributed to the

energy dissipation H_t , present in the denominator of Equation 4. As shown in Figure 2, H_t varies practically linearly with respect to the Froude number, until $F_1 = 3$. Beyond this point, the function behaves hyperbolically: increasing, but in a progressively smaller rate. The equation with best fit is Equation 8, with a coefficient of determination $R^2 = 0.57$.

$$\Omega_{\max} = \frac{F_1}{1080.8 F_1^{0.0047} - 1081.9} \quad (8)$$

Another means of quantifying the turbulence within the hydraulic jump is through the pressure fluctuation coefficient, that was also used by Abdul Khader & Elango (1974), Akbari et al. (1982) and Lopardo (1986) and is presented in Figure 8. In order to describe its behaviour, Equation 9 was derived, which resulted in $R^2 = 0.81$. The data used for validation presented similar values to the proposed equation, notably Lopardo's (1986) and Toso & Bowers' (1988) data. An opposite behaviour that the one of Figure 7 was noticed, i.e., steady jumps present the highest values of pressure fluctuation along the stilling basin. These differences reveal that the analysis of only one dimensionless parameter may induce to an erroneous interpretation of the most critic region of the basin. The combined analysis of these two nondimensionalizations is recommended.

$$C'_p = \frac{1}{0.5 F_1^2 - 6.46 F_1 + 34.9} \quad (9)$$

Position of maximum pressure fluctuation

The results found for the dimensionless longitudinal positions $\Gamma_{\sigma(\max)}$ at which the maximum pressure fluctuations occur, plotted against the Froude number, are visually presented in Figure 9. The maximum pressure fluctuations occur nearer to the basin entrance for higher Froude numbers. The nondimensionalization reveals that the position of maximum pressure fluctuation of undular, weak and oscillating jumps ($F_1 < 4.5$) behaves differently than the one of steady and strong jumps. The function decreases until

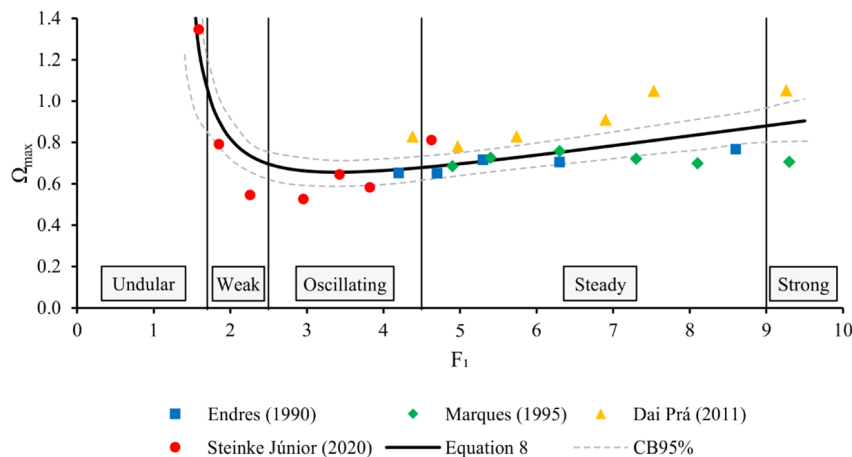


Figure 7. Maximum pressure fluctuation (dimensionless).

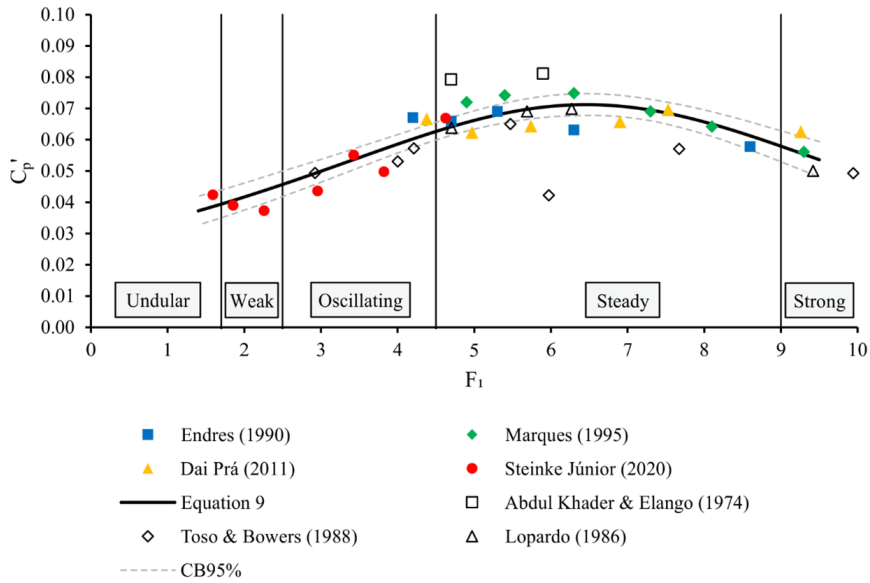


Figure 8. Maximum pressure fluctuation coefficients.

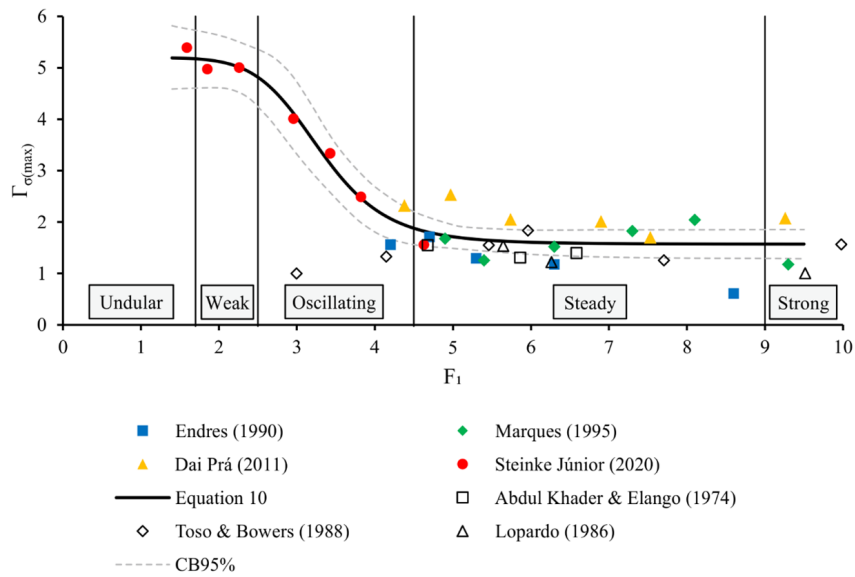


Figure 9. Position of maximum pressure fluctuation (dimensionless).

approximately $F_1 = 4.5$. For the region $F_1 > 4.5$, a plateau zone develops near $\Gamma_{\sigma(\max)} \cong 1.6$. The best fit found is Equation 10 ($R^2 = 0.90$).

Figure 9 and the fitted curve allow to infer that, when it comes to steady and strong jumps, the zone near $\Gamma \cong 1.5$ should receive special attention during design, because it is where the stilling basin slabs will have to withstand the strongest turbulence and, thus, where damages and failures will most likely occur. As for jumps within the $F_1 < 4.5$ range, the region where the highest pressures fluctuations develop depends on the Froude number, and additional experiments in physical models are recommended for a more precise analysis of this region, since the data used for validation are somewhat divergent from the fitted curve.

$$\Gamma_{\sigma(\max)} = \frac{1.6 \times 10^{-4} + 5.197 F_1^{-7.69}}{1.02 \times 10^{-4} + F_1^{-7.69}} \tag{10}$$

Mean pressures at the position of maximum pressure fluctuation

Figure 10 present the dimensionless mean pressures observed at the position where the maximum pressure fluctuation takes place. The data were plotted with respect to the inflow Froude number. The general trend observed is the decrease of Ψ for an increase of F_1 . Equation 11 was adjusted to the point cloud, which resulted in a coefficient of determination $R^2 = 0.89$.

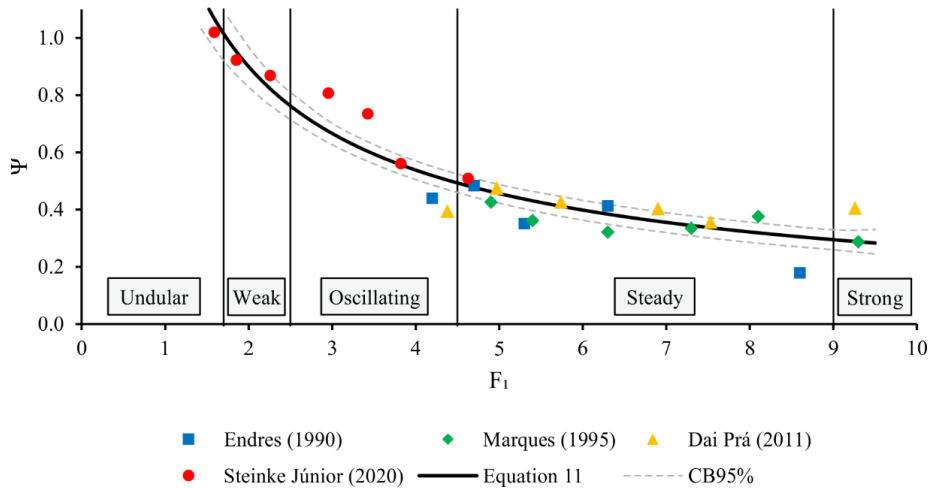


Figure 10. Mean pressures at the position of maximum pressure fluctuation (dimensionless).

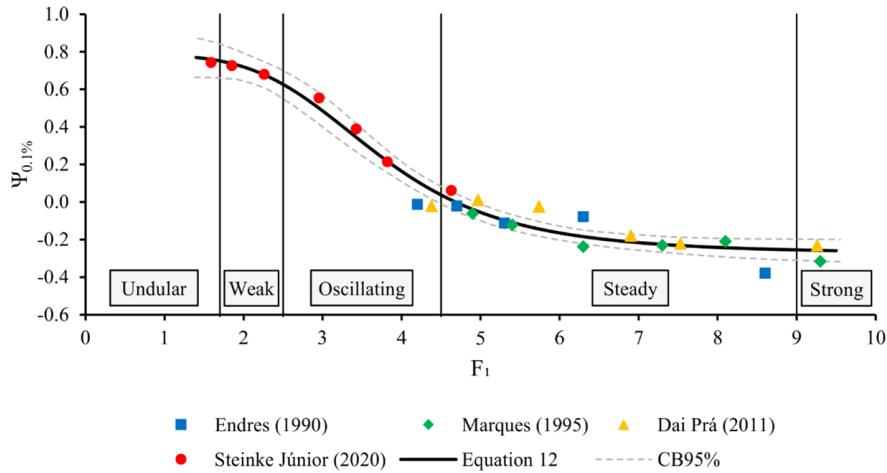


Figure 11. Minimum pressures at the position of maximum pressure fluctuation (dimensionless).

$$\Psi = 1.5 F_1^{-0.74} \quad (11)$$

Minimum pressures $\Psi_{0.1\%}$ at the position of maximum pressure fluctuation

The minimum pressures occurring at the position of maximum pressure fluctuation, made dimensionless using Equation 3, are shown in Figure 11, with respect to the inflow Froude number. The fitted curve, Equation 12 ($R^2 = 0.97$), is also shown in the chart. The data distribution reveals that the extreme minimum pressures of undular, weak and oscillating jumps are generally positive and higher than the inflow sequent depth. Practically speaking, this means that the designer should focus on tensile forces acting on the stilling basin slabs mainly in steady and strong jumps ($F_1 > 4.5$).

$$\Psi_{0.1\%} = \frac{-8 \times 10^{-4} + 0.784 F_1^{-4.46}}{3 \times 10^{-3} + F_1^{-4.46}} \quad (12)$$

The behaviour of the minimum pressures in their dimensional form corroborates this, as can be seen in Figure 12, which presents the data with respect to the inflow Froude number. The data was transformed to prototype scale, using a 1:50 relation for the data of Endres (1990) and Marques (1995). Negative pressures (representing tension on the concrete slabs of the stilling basin) only occur in jumps with $F_1 > 5$, i.e., steady and strong jumps.

Maximum pressures $\Psi_{99.9\%}$ at the position of maximum pressure fluctuation

The maximum pressures at the position of maximum pressure fluctuation are shown in Figure 13, in their dimensionless form. Undular and strong jumps present the highest maximum pressures. Equation 13 was fitted to the point cloud, and resulted in $R^2 = 0.75$.

$$\Psi_{99.9\%} = \frac{F_1}{6.3 F_1^{0.316} - 6} \quad (13)$$

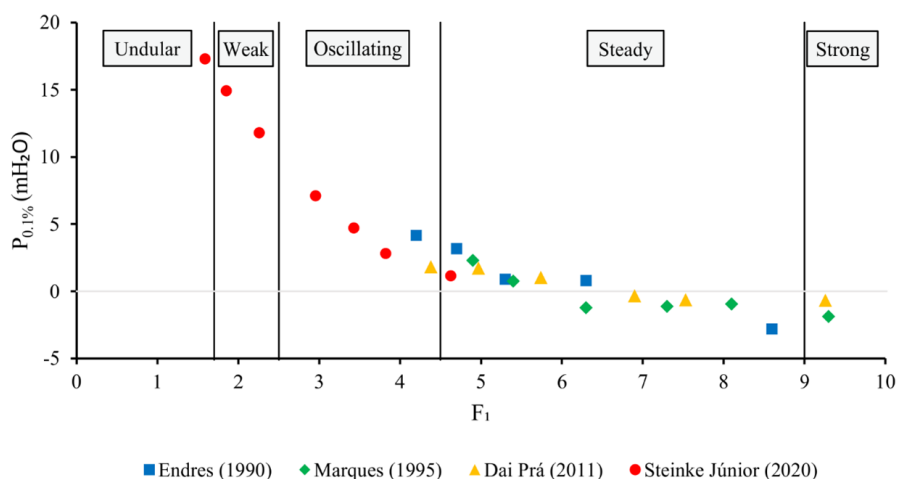


Figure 12. Minimum pressures at the position of maximum pressure fluctuation (dimensional, prototype scale).

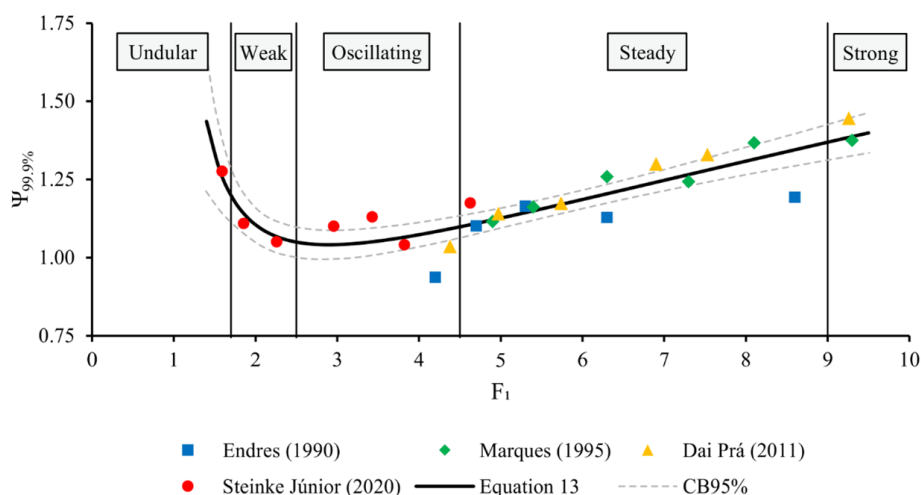


Figure 13. Maximum pressures at the position of maximum pressure fluctuation (dimensionless).

CONCLUSIONS

This study aimed at characterizing the behaviour of mean, minimum and maximum pressures, maximum pressure fluctuations and the position where they occur along the centreline of the stilling basin, as a function of the inflow Froude number. This analysis resulted in a source of information for designers of stilling basins and hydraulic engineers in general. Results show that the most critical minimum pressures (those which may assume negative values) occur in steady and strong jumps. This indicates that undular, weak and oscillating jumps are not likely to incur in damages due to negative pressures. The dimensionless mean pressures at the position of maximum pressure fluctuation were shown to decrease with an increase of the inflow Froude number. This behaviour was also verified for minimum pressures, but not for maximum pressures, which assume higher dimensionless values for undular and strong jumps.

The maximum pressure fluctuations assume the highest values for oscillating, steady and strong jumps. This was shown to be linked with the energy dissipated along the jump, a parameter used for the nondimensionalization. The maximum fluctuations of steady and strong jumps generally occur near the dimensionless position $\Gamma = 2$, while, for other types of hydraulic jump, this metric depends on the Froude number. It is important to highlight that more experimental tests, especially for low Froude numbers, are required for increasing the reliability of the results.

ACKNOWLEDGEMENTS

The authors gratefully acknowledge CNPq, CAPES, the Institute of Hydraulic Research (IPH-UFRGS), Furnas Centrais Elétricas S.A. and Foz do Chapecó Energia S.A. for their support.

Many thanks also to Dr. Endres, Dr. Marques and Dr. Dai Prá for sharing their data.

NOTATION

The following symbols are used in this paper:

C_p' = pressure fluctuation coefficient;
 F_1 = inflow Froude number;
 g = acceleration due to gravity;
 H_t = energy dissipated along jump;
 \bar{P} = mean pressure where σ_{\max} occurs, in equivalent head;
 $P_{0.1\%}$ = extreme pressure 0.1% quantile where σ_{\max} occurs, in equivalent head;
 $P_{99.9\%}$ = extreme pressure 99.9% quantile where σ_{\max} occurs, in equivalent head;
 q = unit flow rate;
 R^2 = coefficient of determination;
 S = submergence factor;
 v_1 = average incident velocity;
 x = longitudinal position, taken from beginning of stilling basin;
 $x_{\sigma(\max)}$ = longitudinal position where σ_{\max} occurs;
 y_1 = supercritical sequent depth;
 y_2 = subcritical sequent depth;
 β = quantile probability;
 Γ = dimensionless longitudinal position;
 $\Gamma_{\sigma(\max)}$ = dimensionless longitudinal position where σ_{\max} occurs;
 Ψ = dimensionless mean pressure;
 $\Psi_{0.1\%}$ = dimensionless extreme pressure quantile for probability 0.1%;
 $\Psi_{99.9\%}$ = dimensionless extreme pressure quantile for probability 99.9%;
 Ω_{\max} = dimensionless standard deviation;
 σ = standard deviation of pressures, in equivalent head (also called pressure fluctuation);
 σ_{\max} = maximum standard deviation of pressures for a given F_1 , in equivalent head (also called maximum pressure fluctuation).

REFERENCES

- Abdul Khader, M. H., & Elango, K. (1974). Turbulent pressure field beneath a hydraulic jump. *Journal of Hydraulic Research*, 12(4), 469-489.
- Akbari, M. E., Mittal, M. K., & Pande, P. K. (1982). Pressure fluctuations on the floor of free and forced hydraulic jumps. In *Proceedings of the International Conference on the Hydraulic Modelling of Civil Engineering Structures*. Coventry: British Hydromechanics Research Association.
- Barjastehmaleki, S., Fiorotto, V., & Caroni, E. (2016). Design of stilling basin linings with sealed and unsealed joints. *Journal of Hydraulic Engineering (New York, N.Y.)*, 142(12), 04016064.
- Bowers, C. E., & Toso, J. (1988). Karnafuli project, model studies of spillway damage. *Journal of Hydraulic Engineering (New York, N.Y.)*, 114(5), 469-483.
- Bowers, C. E., & Tsai, F. Y. (1969). Fluctuating pressures in spillway stilling basins. *Journal of the Hydraulics Division*, 95(6), 2071-2080.
- Bradley, J. N., and Peterka, A. J. (1955). *Progress Report II – Research Study on Stilling Basins, Energy Dissipators, and Associated Appurtenances* (N° Hyd-399, Bureau of Reclamation Hydraulic Laboratory Report). Denver: Commissioner's Office.
- Chow, V. T. (1959). *Open channel hydraulics*. New York: McGraw-Hill.
- Dai Prá, M. (2011). *Uma abordagem para determinação das pressões junto ao fundo de dissipadores de energia por ressalto hidráulico* (Tese de doutorado). Instituto de Pesquisas Hidráulicas, Universidade Federal do Rio Grande do Sul, Porto Alegre.
- Elevatorski, E. A. (1959). *Hydraulic energy dissipators*. New York: McGraw-Hill.
- Endres, L. A. M. (1990). *Contribuição ao desenvolvimento de um sistema para aquisição e tratamento de dados de pressões instantâneas em laboratório* (M.Sc. dissertation). Instituto de Pesquisas Hidráulicas, Universidade Federal do Rio Grande do Sul, Porto Alegre.
- Fiorotto, V., & Rinaldo, A. (1992). Fluctuating uplift and lining design in spillway stilling basins. *Journal of Hydraulic Engineering (New York, N.Y.)*, 118(4), 578-596.
- Fiorotto, V., & Salandin, P. (2000). Design of anchored slabs in spillway stilling basins. *Journal of Hydraulic Engineering (New York, N.Y.)*, 126(7), 502-512.
- Hassanpour, N., Hosseinzadeh Dalir, A., Bayon, A., & Abdollahpour, M. (2021). Pressure fluctuations in the spatial hydraulic jump in stilling basins with different expansion ratio. *Water (Basel)*, 13(1), 60.
- Jesudhas, V., Balachandar, R., Roussinova, V., & Barron, R. (2018). Turbulence characteristics of classical hydraulic jump using DES. *Journal of Hydraulic Engineering (New York, N.Y.)*, 144(6), 04018022.
- King, D. L. (1967). Analysis of random pressure fluctuations in stilling basins. In *Proceedings of the XII Congress of the International Association for Hydraulic Research*. Fort Collins: IAHR.
- Lopardo, R. A. (1985). Metodología de estimación de presiones instantâneas en cuencos amortiguadores. *Anales de La Universidad de Chile*, 5(8), 437-455.
- Lopardo, R. A. (1986). *Notas sobre fluctuaciones macroturbulentas de presión, medición, análisis y aplicación al resalto hidráulico* (Curso n. 1: Turbulencia, cavitación y aireación de fenómenos hidráulicos). São Paulo: Escola Politécnica.
- Lopardo, R. A. (2002). Contribution of hydraulic models on the safe design of large dams stilling basins. In *Proceedings of the IAHR Symposium on Hydraulic and Hydrological Aspects of Reliability and Safety Assessment of Hydraulic Structures*. St. Petersburg: IAHR.
- Macián-Pérez, J. F., Bayon, A., García-Bartual, R., Amparo López-Jiménez, P., & Vallés-Morán, F. J. (2020). Characterization of structural properties in high Reynolds hydraulic jump based

- on CFD and physical modeling approaches. *Journal of Hydraulic Engineering (New York, N.Y.)*, 146(12), 04020079.
- Maleki, S., & Fiorotto, V. (2021). Hydraulic jump stilling basin design over rough beds. *Journal of Hydraulic Engineering (New York, N.Y.)*, 147(1), 04020087.
- Marques, M. G. (1995). *Nouvelle approche pour le dimensionnement des dissipateurs à auge*. Ph.D. thesis. Departement de Génie Civil, Université Laval, Québec.
- Marques, M. G., Hampe, R. F., Souza, P. E. A., & Teixeira, E. D. (2017). Previsão de pressões extremas mínimas em bacia de dissipação com baixo número de Froude. In *Anais do XXXI Seminário Nacional de Grandes Barragens*. Belo Horizonte: CBDB.
- Marques, M. G., Drapeau, J., & Verrette, J.-L. (1997). Flutuação de pressão em um ressalto hidráulico. *RBRH*, 2(2), 45-52.
- Mees, A. A. A. (2008). *Caracterização das solicitações hidrodinâmicas em bacias de dissipação por ressalto hidráulico com baixo número de Froude* (Dissertação de mestrado). Instituto de Pesquisas Hidráulicas, Universidade Federal do Rio Grande do Sul, Porto Alegre.
- Peterka, A. J. (1984). *Hydraulic design of stilling basins and energy dissipators*. Denver: USBR.
- Pfister, M., & Hager, W. H. (2010). Chute aerators. I: Air transport characteristics. *Journal of Hydraulic Engineering (New York, N.Y.)*, 136(6), 352-359. [http://dx.doi.org/10.1061/\(ASCE\)HY.1943-7900.0000189](http://dx.doi.org/10.1061/(ASCE)HY.1943-7900.0000189).
- Şentürk, F. (1994). *Hydraulics of dams and reservoirs*. Littleton: Water Resources Publications.
- Steinke Júnior, R. (2020). *Caracterização das pressões em bacias de dissipação por ressalto hidráulico livre com baixo número de Froude* (Dissertação de mestrado). Instituto de Pesquisas Hidráulicas, Universidade Federal do Rio Grande do Sul, Porto Alegre.
- Steinke Júnior, R., Dai Prá, M., Lopardo, R. A., Marques, M. G., Melo, J. F., Priebe, P. S., & Teixeira, E. D. (2021). Low froude number stilling basins: hydrodynamic characterization. *Journal of Hydraulic Engineering (New York, N.Y.)*, 147(4), 04021010.
- Stojnic, I., Pfister, M., Matos, J., & Schleiss, A. J. (2021). Effect of 30-degree sloping smooth and stepped chute approach flow on the performance of a classical stilling basin. *Journal of Hydraulic Engineering (New York, N.Y.)*, 147(2), 04020097.
- Teixeira, E. D. (2008). *Efeito de escala na previsão dos valores extremos de pressão junto ao fundo em bacias de dissipação por ressalto hidráulico* (Tese de doutorado). Instituto de Pesquisas Hidráulicas, Universidade Federal do Rio Grande do Sul, Porto Alegre.
- TEMELSU. (2022). *Engineering Services for Remedial Structures on the Spillway of Keban Dam—Turkey*. Retrieved in 2022, April 18, from <http://en.temelsu.net/engineering-services-for-remedial-structures-on-the-spillway-of-keban-dam/>
- Toso, J. W., & Bowers, E. (1988). Extreme pressures in hydraulic-jump stilling basins. *Journal of Hydraulic Engineering (New York, N.Y.)*, 114(8), 829-843.
- Vasiliev, O. F., & Bukreyev, V. I. (1967). Statistical characteristics of pressure fluctuations in the region of hydraulic jump. In *Proceedings of the XII Congress of the International Association for Hydraulic Research*. Fort Collins: IAHR.
- Witt, A., Gulliver, J. S., & Shen, L. (2018). Numerical investigation of vorticity and bubble clustering in an air entraining hydraulic jump. *Computers & Fluids*, 172, 162-180.

Authors contributions

Renato Steinke Júnior.: Performed the methodology, obtained the results and wrote the text.

Priscila Maria Kipper: Performed the methodology, obtained the results and wrote, formatted and revised the text.

Leandro Broch Ferreira: Performed the methodology, obtained the results and wrote the text.

Eder Daniel Teixeira: Contributed with technical notes and revised the text.

Mauricio Dai Prá: Contributed with technical notes and revised the text.

Marcelo Giulian Marques: Defined the objectives, contributed with technical notes, revised the text and the results.

Editor in-Chief: Adilson Pinheiro

Associated Editor: Iran Eduardo Lima Neto